Available online at www.sciencedirect.com

ScienceDirect

Mendeleev Commun., 2019, **29**, 512–514

Mendeleev Communications

UVC-induced photodegradation of *p*-arsanilic acid assisted by humic substances

Yuliya E. Tyutereva,[a,b] Peter S. Sherin,[a,c] Zizheng Liu,[d] Victor F. Plyusnin[a,b] and Ivan P. Pozdnyakov*[a,b]

[a] *Novosibirsk State University, 630090 Novosibirsk, Russian Federation*
[b] *V. V. Voevodsky Institute of Chemical Kinetics and Combustion, Siberian Branch of the Russian Academy of Sciences, 630090 Novosibirsk, Russian Federation. E-mail: pozdnyak@kinetics.nsc.ru*
[c] *International Tomography Center, Siberian Branch of the Russian Academy of Sciences, 630090 Novosibirsk, Russian Federation*
[d] *School of Civil Engineering, Wuhan University, 430079 Wuhan, China*

DOI: 10.1016/j.mencom.2019.09.011

Quantum yields of indirect UVC photodegradation of *p*-arsanilic acid (a widely used phenylarsonic feed additive) caused by the photolysis of humic substances were measured. The acquired results demonstrate that the efficiency of such decomposition of *p*-arsanilic acid is comparable with that of its direct UVC photolysis due to the participation of active intermediates generated during the photolysis of humic substances. These results could be important for understanding the fate of *p*-arsanilic acid during an UVC disinfection of wastewaters containing natural humic substances.

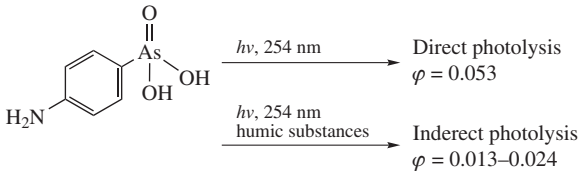

Humic substances (HSs, including humic and fulvic acids) are naturally occurring photoactive components, which are widely present in surface waters.[1] Under solar irradiation, these compounds generate different active intermediates (triplet states, hydrated electrons, and reactive oxygen species), which can react with dissolved organic pollutants initiating their degradation and mineralization.[1–3] On the other hand, the presence of HSs could increase the pollutant photostability due to the competition for the light quanta with the target compound.[4,5] The total effect of HSs depends on the absorbance and quantum yield of photolysis of both HSs and target pollutant at applied excitation wavelengths.[4–8] It should be emphasized that most researchers limit themselves by measurements of relative efficiency of pollutants degradation in the presence of HSs (*i.e.*, rate constants of the photolysis), while they rarely provide the values of absolute efficiency (quantum yield) of photolysis. This significantly complicates a correct estimation of HSs influence on the efficiency of target pollutant photodegradation in both natural waters and during wastewater treatment procedures.

The present work was aimed at clarifying the influence of HSs on UVC-induced photodegradation of *p*-arsanilic acid (*p*-ASA)[†] that is a phenylarsonic feed additive used widely in the livestock and poultry industries as antibiotics to promote animal growth.[9,10] Although *p*-ASA possesses a low toxicity, products of its biological and (photo)chemical degradation, inorganic arsenic compounds and other organic by-products, exhibit significant toxicity to the natural environment.[11,12] The major issues were the determination of absolute efficiency (quantum yields) of HSs-assisted photodegradation of *p*-ASA and preliminary identification of main intermediate(s) involved in the photoprocesses.

Figure 1 shows absorption spectra of *p*-ASA solution during its photolysis at 254 nm in the absence of HS. Three maxima (218, 300 and 525 nm), two minima (203 and 250 nm), and three isosbestic points (211, 232 and 271 nm) are clearly seen in the differential absorption spectra (see Figure 1, inset). The results are similar to those observed in our recent work.[14] Using HPLC data on the *p*-ASA degradation during the photolysis,[14] were plotted the curves of concentration of photodegraded *p*-ASA ($-\Delta$[*p*-ASA]) *vs.* changes of optical density at 252 nm ($-\Delta A_{252}$) together with the best polynomial fit (Figure S2, see Online Supplementary Materials). This

[†] *p*-ASA ($C_6H_8AsNO_3$, 98%, Aladdin Industrial Corporation, China), fulvic acid from Henan ChangSheng Corporation, China (CS), Nordic Lake fulvic acid (NL, IHSS reference 1R105F, USA), and fulvic acid from Aladdin Industrial Corporation, China (AL, H108498, CAS: 1415-93-6) were used without additional purification. The pH value was controlled using an ANION-4100 ion-meter (LTD Infraspak-Analit, Russia) equipped with an ESK-10614 combined electrode. NaOH or $HClO_4$ of analytical grade were used for pH adjustments. Deionized water was used for the preparation of solutions.

Unless otherwise noted, the concentration of *p*-ASA was 10^{-5} mol dm^{-3}, while the concentration of HS was varied from 1 to 10 mg dm^{-3} (see Figure S1, Online Supplementary Materials). The initial pH of solutions was in the range of 6.7–7.6 depending on the used type of fulvic acid, corresponding to almost 100% monoanionic form of *p*-ASA.[13] The concentration of *p*-ASA during its photolysis was measured using a LC 1200 high performance liquid chromatography (HPLC) system (Agilent Technologies, USA) equipped with a diode array detector as was previously reported.[14]

UV-VIS spectra were recorded using an Agilent 8453 spectrophotometer (Agilent Technologies). An UVC ozone-free Radium Puritec lamp (9 W, OSRAM GmbH, Germany) emitting at 254 nm was used as the source of steady-state irradiation. All the stationary photolysis experiments were carried out in quartz cells possessing an optical path of 5 cm and a total volume of 0.01 dm^{-3} at 298 K under atmospheric pressure. To provide uniform excitation of the samples, a magnetic stirrer was used during the irradiation. To calculate the *p*-ASA photodegradation rates and quantum yields, the lamp intensity (4 mV cm^{-2}) was determined using a ferrioxalate actinometer in the photochemical cell analogous to a previously reported one.[14] All the values are averages of duplicate or triplicate experiments.

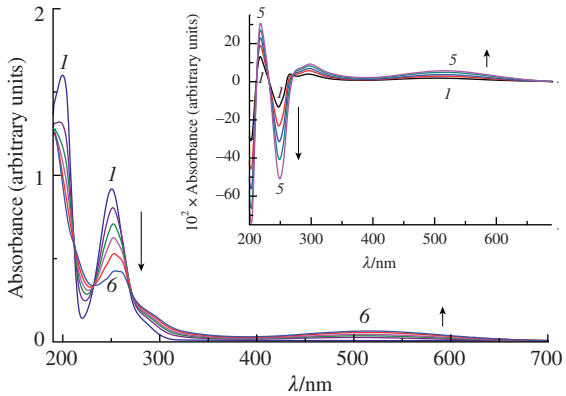

Figure 1 Absorption spectra of *p*-ASA (10^{-5} mol dm^{-3}) after (*1*) 0, (*2*) 3, (*3*) 5, (*4*) 7, (*5*) 10 and (*6*) 15 min of steady-state (254 nm) photolysis. The inset shows differential absorption spectra (subtraction of absorption spectrum at 0 min) after (*1*) 3, (*2*) 5, (*3*) 7, (*4*) 10 and (*5*) 15 min of photolysis.

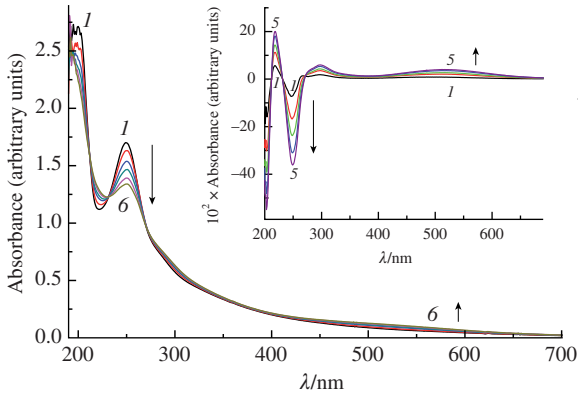

Figure 2 Absorption spectra of *p*-ASA (10^{-5} mol dm^{-3}) in the presence of AL (4.5 mg dm^{-3}) after (*1*) 0, (*2*) 2, (*3*) 4, (*4*) 6, (*5*) 8 and (*6*) 10 min of steady-state (254 nm) photolysis. The inset shows differential absorption spectra (subtraction of absorption spectrum at 0 min) after (*1*) 2, (*2*) 4, (*3*) 6, (*4*) 8 and (*5*) 10 min of photolysis.

calibration curve allowed us to further measure the rate of *p*-ASA disappearance using the optical spectroscopy instead of more time consuming HPLC technique.

Figure 2 depicts the absorption spectra of *p*-ASA solution during photolysis at 254 nm in the presence of fulvic acid (of AL type). Differential absorption spectra (see Figure 2, inset) demonstrate the same maxima, minima and isosbestic points as in the case of pure *p*-ASA photolysis (see Figure 1, inset). For all other HSs, the changes in differential absorption spectra of irradiated mixture of HSs and *p*-ASA were qualitatively the same as for irradiated *p*-ASA in the absence of HSs (these data are not shown). The presence of HSs affects only the rate of *p*-ASA photodegradation. It means that the presence of HSs does not change the set of *p*-ASA photoproducts and allows one to calculate the *p*-ASA photolysis rate in the presence of HSs using the calibration curve (Figure S2). It is worth to note that HSs solutions were quite stable upon irradiation at 254 nm (Figure S3), and it was possible to neglect changes in HSs absorbance at the initial stage of photolysis used for the measurement of *p*-ASA photolysis rate (typically, 10 min).

The ratio of the rate of *p*-ASA photolysis in the presence of HSs (r) to that in the absence of HSs (r_0) could be expressed as (see Online Supplementary Materials for details):

$$\frac{r}{r_0} = \frac{A_{ASA} + (\gamma_{ASA}\phi_{HS}/\phi_{ASA})A_{HS}}{A_{ASA} + A_{HS}} \frac{1 - 10^{-(A_{ASA}+A_{HS})}}{1 - 10^{-A_{ASA}}}, \quad (1)$$

where φ_{ASA} and φ_{HS} are quantum yields of direct *p*-ASA and HS photolysis, respectively; A_{ASA} and A_{HS} are initial absorbance of *p*-ASA and HS at 254 nm, respectively; γ_{ASA} is the probability for active species generated by HS photolysis to react with *p*-ASA. The value of γ_{ASA} depends generally on [*p*-ASA], so the total efficiency of indirect HSs-assisted photolysis could be reduced upon the decreased *p*-ASA concentration.[15]

In equation (1), there is only one unknown parameter ($\gamma_{ASA}\varphi_{HS}$). In our previous work,[14] the value of $\varphi_{ASA} = 0.053$ was estimated by the HPLC analysis of photolyzed samples. The value of A_{ASA} is the fixed parameter determined by the initial concentration of *p*-ASA, and A_{HS} is a varying parameter calculated from the absorption spectra of *p*-ASA–HSs mixtures (see Figure 2). Figure 3 demonstrates r/r_0 ratios at the different initial absorbance of HS at 254 nm. The initial rates of *p*-ASA photolysis were calculated using linear fits of changes in the *p*-ASA concentration during the first 10 min of photolysis (Figure S4). For all the used HSs, the experimental values (points) exceeded the theoretical value obtained according to equation (1) for $\gamma_{ASA}\varphi_{HS} = 0$ (dotted line). This means that the HS actively participates in the *p*-ASA photodegradation upon its exposure to the irradiation at 254 nm. The best agreement between experimental data and equation (1) was obtained for the $\gamma_{ASA}\varphi_{HS}$ values of 2.4±0.4, 1.9±0.3 and 1.2±0.2% for CS, AL and NL substances, respectively. All the obtained $\gamma_{ASA}\varphi_{HS}$ values are comparable with the value for direct *p*-ASA photolysis (φ_{ASA} = 5.3±0.5%).

It is known that the UV excitation of HSs leads to the generation of several primary species, such as the triplet state (^{3}HS), the hydrated electron (e^-_{aq}), and the radical cation ($HS^{\cdot+}$).[1,16–18] The two first intermediates react rapidly with dissolved oxygen to form singlet oxygen ($^1O_2$) and superoxide anion radical ($O_2^{\cdot-}$), respectively.

$$HS \xrightarrow{h\nu} HS^{\cdot+} + e^-_{aq} \quad (2)$$

$$HS \xrightarrow{h\nu} {}^3HS \quad (3)$$

$$e^-_{aq} + O_2 \longrightarrow O_2^{\cdot-} \ (k = 2\times10^{10} \text{ dm}^3 \text{ mol}^{-1} \text{ s}^{-1})^{19} \quad (4)$$

$$^3HS + O_2 \longrightarrow {}^1O_2 + HS \ (k \approx 10^9 \text{ dm}^3 \text{ mol}^{-1} \text{ s}^{-1})^{16} \quad (5)$$

Since the low (10^{-5} mol dm^{-3}) concentration of *p*-ASA was used in this work, the reaction of *p*-ASA with primary HSs intermediates could not compete with the reactions (4) and (5) even at the limited value of diffusion for these processes (6×10^9 dm^3 mol^{-1} s^{-1} in aqueous solution). Thus, the indirect photolysis of *p*-ASA in the presence of HSs has to be determined by $HS^{\cdot+}$ and secondary intermediates of HSs photochemistry, such as $^1O_2$ and $O_2^{\cdot-}$. The rate constant of *p*-ASA reaction with singlet oxygen is known (2.4×10^6 dm^3 mol^{-1} s^{-1}).[14] Since the $^1O_2$ lifetime in water is 3.1 μs,[20] this reaction is negligible at the *p*-ASA concentration lower than 10^{-3} mol dm^{-3}. The yields of $O_2^{\cdot-}$ and $HS^{\cdot+}$ could be determined *via* measuring the yield of hydrated electron in laser flash photolysis experiments by its characteristic absorption at

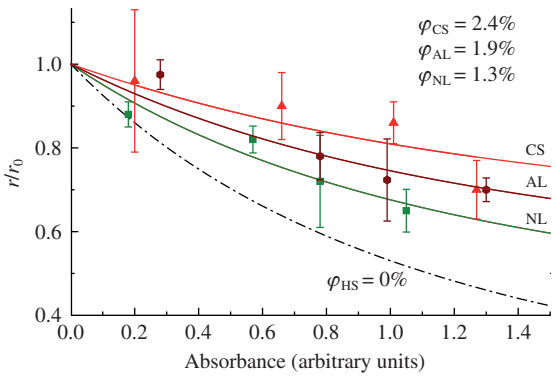

Figure 3 Values of r/r_0 ratios (points) at the different initial absorbance of HSs at 254 nm. Solid curves are the best fits according to equation (1) for the shown φ_{HS} values. The dotted curve is the reference one calculated by equation (1) for $\varphi_{HS} = 0$.

720 nm. However, these experiments were out of scope of this preliminary study, thus remaining a subject of further work.

In conclusion, the presence of highly absorbing HSs does not significantly reduce the efficiency of UVC-induced photolysis of *p*-ASA due to the participation of active intermediates generated during the HS photolysis in the *p*-ASA photodegradation. The nature of these intermediates ($O_2^{\cdot-}$ and $HS^{\cdot+}$, most probably) has to be proven by further laser flash photolysis experiments. The quantum yields of *p*-ASA HSs-assisted photolysis (at [*p*-ASA] = = 10^{-5} mol dm^{-3}) upon excitation at 254 nm ($\gamma_{ASA}\varphi_{HS}$) are in the range of 1.3–2.4% and comparable with the quantum yield of direct *p*-ASA photolysis (5.3%). Additional measurements of $\gamma_{ASA}\varphi_{HS}$ values at a lower concentration of *p*-ASA are also needed in order to estimate the influence of HS on the indirect *p*-ASA photolysis under environmentally relevant conditions. These data are important for understanding the fate of *p*-ASA in the presence of HSs during a wastewater disinfection.

This work was supported by the Russian Foundation for Basic Research (grant nos. 18-53-53006_GFEN and 18-53-00002_BEL) and the National Natural Science Foundation of China and the Russian Foundation for Basic Research (grant no. NSFC-RFBR 51811530099). The authors are grateful to the Ministry of Science and Higher Education of Russian Federation for access to HPLC equipment (project no. AAAA-A16-116121510087-5).

Online Supplementary Materials

Supplementary data associated with this article can be found in the online version at doi: 10.1016/j.mencom.2019.09.011.

References

1 K. McNeill and S. Canonica, *Environ. Sci.: Processes Impacts*, 2016, **18**, 1381.
2 N. V. Blough and R. G. Zepp, in *Active Oxygen in Chemistry*, eds. C. S. Foote, J. S. Valentine, A. Greenberg and J. F. Liebman, Chapman and Hall, New York, 1995, ch. 8, pp. 280–333.
3 N. B. Sul'timova, P. P. Levin, O. N. Chaikovskaya and I. V. Sokolova, *High Energy Chem.*, 2008, **42**, 464 (*Khim. Vys. Energ.*, 2008, **42**, 514).
4 M. Kepczyński, A. Czosnyka and M. Nowakowska, *J. Photochem. Photobiol., A*, 2007, **185**, 198.
5 Y. Si, J. Zhou, H. Chen, D. Zhou and Y. Yue, *Chemosphere*, 2004, **56**, 967.
6 D. Vialaton, C. Richard, D. Baglio and A.-B. Paya-Perez, *J. Photochem. Photobiol., A*, 1998, **119**, 39.
7 H. Xu, W. J. Cooper, J. Jung and W. Song, *Water Res.*, 2011, **45**, 632.
8 I. P. Pozdnyakov, V. A. Salomatova, M. V. Parkhats, B. M. Dzhagarov and N. M. Bazhin, *Mendeleev Commun.*, 2017, **27**, 399.
9 F. T. Jones, *Poult. Sci.*, 2007, **86**, 2.
10 E. K. Silbergeld and K. Nachman, *Ann. N. Y. Acad. Sci.*, 2008, **1140**, 346.
11 I. Cortinas, J. A. Field, M. Kopplin, J. R. Garbarino, A. J. Gandolfi and R. Sierra-Alvarez, *Environ. Sci. Technol.*, 2006, **40**, 2951.
12 K. C. Makris, S. Quazi, P. Punamiya, D. Sarkar and R. Datta, *Environ. Qual.*, 2008, **37**, 1626.
13 J. Jaafar, *J. Teknol.*, 2001, **35**, 71.
14 Yu. E. Tyutereva, P. S. Sherin, M. V. Parkhats, Z. Liu, J. Xu, F. Wu, V. F. Plyusnin and I. P. Pozdnyakov, *Chemosphere*, 2019, **220**, 574.
15 I. P. Pozdnyakov, P. S. Sherin, V. A. Salomatova, M. V. Parkhats, V. P. Grivin, B. M. Dzhagarov, N. M. Bazhin and V. F. Plyusnin, *Environ. Sci. Pollut. Res.*, 2018, **25**, 20320.
16 M. P. Makunina, I. P. Pozdnyakov, V. P. Grivin and V. F. Plyusnin, *High Energy Chem.*, 2014, **48**, 197 (*Khim. Vys. Energ.*, 2014, **48**, 236).
17 J. P. Aguer, C. Richard and F. Andreux, *Analysis*, 1999, **27**, 387.
18 J. F. Power, D. K. Sharma, C. H. Langford, R. Bonneau and J. Joussot-Dubien, *Photochem. Photobiol.*, 1986, **44**, 11.
19 G. V. Buxton, C. L. Greenstock, W. P. Helman and A. B. Ross, *J. Phys. Chem. Ref. Data*, 1988, **17**, 513.
20 C. Schweitzer and R. Schmidt, *Chem. Rev.*, 2003, **103**, 1685.

Received: 13th February 2019; Com. 19/5828